

# Graphene oxide for diode-pumped Tm:YLF passively *Q*-switched laser at 2 $\mu\text{m}$

Yuqian Zu (祖玉倩)<sup>1</sup>, Cheng Zhang (张程)<sup>1</sup>, Yongjing Wu (吴永静)<sup>1</sup>, Jingjing Liu (刘晶晶)<sup>1</sup>,  
Jie Liu (刘杰)<sup>1,2,\*</sup>, and Yonggang Wang (王勇刚)<sup>3</sup>

<sup>1</sup>Shandong Provincial Key Laboratory of Optics and Photonic Device, School of Physics and Electronics, Shandong Normal University, Jinan 250014, China

<sup>2</sup>Institute of Data Science and Technology, Shandong Normal University, Jinan 250014, China

<sup>3</sup>School of Physics and Information Technology, Shaanxi Normal University, Xi'an 710119, China

\*Corresponding author: jieliu@sdsu.edu.cn

Received October 1, 2017; accepted November 23, 2017; posted online January 31, 2018

A diode-pumped Tm:YLF passively *Q*-switched laser at 2  $\mu\text{m}$  was first demonstrated by using graphene oxide (GO) as a saturable absorber (SA). In this letter, continuous-wave (CW) laser and pulse laser performances were studied meticulously and systematically. It reasonably showed the dependence of the pulse duration, pulse energy, and pulse repetition rate on the absorbed power. A maximum repetition rate of 38.33 kHz and a single pulse energy of 9.89  $\mu\text{J}$  were obtained.

OCIS codes: 140.3380, 140.3480, 140.3540, 160.4330.  
doi: 10.3788/COL201816.020013.

*Q*-switched diode-pumped solid-state lasers operating in the eye-safe spectral range near 2  $\mu\text{m}$  have attracted attention owing to their potential applications in medical surgery (due to strong absorption of water), environmental atmosphere monitoring, laser ranging, and pumping sources for mid-infrared optical parametric oscillators (OPOs)<sup>[1,2]</sup>. The rare-earth-ion Tm<sup>3+</sup> and Ho<sup>3+</sup>-doped materials have become the mature materials for 2  $\mu\text{m}$  wave band lasers. In particular, Tm<sup>3+</sup> ions have long fluorescence lifetime, high quantum efficiency, and an absorption band that matches well with GaAs/AlGaAs laser diodes near 790 nm<sup>[3]</sup>. Lots of thulium-doped crystals have been recognized as very interesting active media for diode-pumped 2  $\mu\text{m}$  laser such as Tm:YAG, Tm:YLF, and Tm:YAP<sup>[2-5]</sup>. The traditional ways to achieve passively *Q*-switched lasers are to rely on different materials as saturable absorbers (SAs) such as those based on zinc chalcogenides, Cr:ZnS, and Cr:ZnSe<sup>[6-8]</sup>. In recent years, two-dimensional (2D) materials as a novel kind of SAs bring new opportunities for pulse lasers. 2D materials such as graphene, graphene oxide (GO), carbon nanotube, transition metal dichalcogenides, and topological insulators have been widely investigated for 2  $\mu\text{m}$  pulse lasers<sup>[1-3,9-12]</sup>.

Focusing on GO, the addition of hydroxyl, epoxy, and carboxyl groups to the quasi-2D lattice of graphene leads to the creation of GO<sup>[13,14]</sup>. For graphene, atoms of carbon are arranged in a 2D honeycomb lattice with a nearest neighbor distance of about 1.42  $\text{\AA}$ <sup>[15]</sup>. Graphene behaves like a zero-gap semiconductor, and the absorption of graphene is independent of optical frequency<sup>[16-18]</sup>. Therefore, graphene is a suitable absorber for many lasers at a wide range of wavelengths. Graphene is emerging as an ultra-broadband SA for the near-IR, with beneficial properties including high optical transparency, ultrafast saturable absorption, fast recovery time, and moderate modulation

depth<sup>[10,17,19]</sup>. However, it is difficult to grow graphene film with high quality, which makes graphene absorbers expensive. Furthermore, graphene cannot be dissolved in water, so the efficiency for film fabrication by graphene aqueous solution is decreased<sup>[20,21]</sup>. For GO, served as a precursor for graphene, its nanosheets can be readily dispersed in water for the carboxyl and hydroxyl groups in its structure, which leads to a higher deposition efficiency in the vertical evaporation method<sup>[20,22]</sup>. Because of this, GO has its own unique advantages such as low cost and simple fabrication method<sup>[14,19,22,23]</sup>. Compared to graphene, GO has different optoelectronic properties; however, its nonlinear saturable absorption performance is almost comparable to that of graphene<sup>[14,20,23,24]</sup>. It possesses saturable absorption in a broad spectral range (from 800 to 2000 nm) that makes it suitable for passively *Q*-switched and mode-locked multiwavelength lasers<sup>[19]</sup>. Recently, GO-based passively *Q*-switched and mode-locked fiber lasers have been demonstrated in Er-doped, Yb-doped, Tm-doped, and Tm-Ho-codoped<sup>[21-24]</sup> fiber lasers, respectively<sup>[14,24,25]</sup>. GO-based solid-state diode-pumped passively *Q*-switched and mode-locked lasers at 1  $\mu\text{m}$  have also been widely reported<sup>[19,20,22,26]</sup>. In 2012, Feng *et al.*<sup>[2]</sup> have achieved a diode-pumped Tm:YAP, solid-state *Q*-switched mode-locked (QML) laser by using a GO SA (GOSA). In the same year, Liu *et al.*<sup>[5]</sup> have demonstrated the GO as an SA in the passive mode-locking of a diode-pumped Tm:YAP laser. From Refs. [2,5], we can see that GO as an SA in solid-state diode-pumped *Q*-switched or mode-locked 2  $\mu\text{m}$  lasers have shown excellent saturable absorption performance. But, for 2  $\mu\text{m}$  lasers, there are few reports on the solid-state diode-pumped *Q*-switched or mode-locked lasers with GO SAs.

Tm:YLF crystal is a low-phonon material. Compared with other crystals, it has many advantages, such as no heat induced dual refraction, small conversion loss, and

output light polarization. The Tm:YLF crystal has absorption band at 792–793 nm and emission band at 1850–2000 nm<sup>[27]</sup>. For Tm:YLF, the passive  $Q$ -switching based conventional SAs<sup>[28–31]</sup> and active  $Q$ -switching based acousto-optic modulators have been widely studied<sup>[32–34]</sup>. In recent years, the emergence of 2D materials has brought new opportunities to the study of the pulsed laser characteristics of the Tm:YLF crystal. GO as a typical 2D material has shown excellent advantages including feasible saturable absorption band, fast recovery time and moderate modulation depth in compared with the conventional SAs and acousto-optic modulators, thus allowing for generating short pulse laser in a compact way, while the acousto-optic modulators restrict the compactness of  $Q$ -switched lasers. However, the diode-pumped passively  $Q$ -switched and mode-locked reports of the Tm:YLF crystal based on 2D materials are very rare<sup>[12]</sup>.

In this letter, by using GO as an SA, a compact passively  $Q$ -switched diode-pumped Tm:YLF laser was demonstrated for the first time. When the absorbed pump power reached 1.415 W, the stably passively  $Q$ -switched operation was realized. Under the absorbed pump power of 4.44 W, the maximum repetition rate was 38.33 kHz, while the shortest pulse width was 1.038  $\mu$ s and the single pulse energy was 9.89  $\mu$ J. Our results reveal that GO is suitable and promising to be applied in 2  $\mu$ m diode-pumped passively  $Q$ -switched and mode-locked lasers.

The GO sheet used in this experiment was fabricated using ultrasonic agitation following a chemical oxidation of the graphite. The specific preparation method and the characterization of the GO were described in detail in Ref. [5]. The saturable absorption, i.e., the optical intensity required in a steady state to reduce the absorption to half of its unbleached value<sup>[35]</sup>, is also termed the modulation depth, and is very important in evaluating the pulse shaping abilities of SAs. We quoted a model<sup>[36]</sup>

$$T(I) = 1 - \varphi_0 \times \exp(-I/I_{\text{sat}}) - \varphi_{\text{ns}}, \quad (1)$$

to characterize the nonlinear optical curve [ $T(I)$ ,  $\varphi_0$ ,  $I$ ,  $I_{\text{sat}}$ , and  $\varphi_{\text{ns}}$  correspond to transmission, modulation depth, input optical intensity, saturation optical intensity, and nonsaturable loss, respectively]. The nonlinear transmission of the GO is shown in Fig. 1. The source used was a homemade 23.66 ps pulse fiber laser with a repetition rate of 31 MHz at 2000 nm. The resulting GOSA had a modulation depth of 23.1% and a nonsaturable loss of 35.2%. Serres *et al.* reported the modulation depth of the SA was 1.2%<sup>[1]</sup>. Therefore our modulation depth was relatively large, which was attributed to the fact that the thickness and concentration of our SA can be chosen flexibly. In terms of laser performance, the larger modulation depth of GO ensures long term stability of the generated laser pulses by avoiding pulse splitting<sup>[35]</sup>.

The schematic of the Tm:YLF passively  $Q$ -switched laser is shown in Fig. 2. The pump source was a fiber-coupled 793 nm diode laser with a core diameter of 400  $\mu$ m and a numerical aperture of 0.22. The pump laser

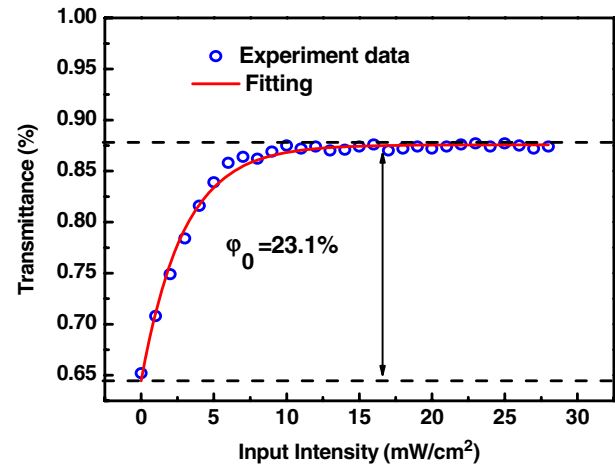


Fig. 1. Nonlinear transmission of the GO saturable absorber.

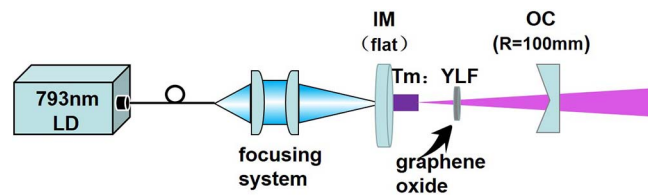


Fig. 2. Schematic of the Tm:YLF laser passively  $Q$ -switched with GO as a saturable absorber.

was focused on the gain medium via a 1:0.5 coupling system to a spot radius of about 100  $\mu$ m. A c-cut, 3 at.-%-doped Tm:YLF crystal was used as the laser gain medium with dimensions of 3 mm  $\times$  3 mm  $\times$  8 mm. Its sides were antireflection coated for 790–795 nm and 1910 nm, respectively. The crystal was wrapped with indium foil and mounted in a copper heat sink cooled by water at 15°C.

A 38 mm straight plane-concave cavity consisted of a plane mirror (IM) and a concave mirror was constructed. The plane mirror has a high transmission at 780–810 nm and high reflection at 1900–2000 nm. The concave mirror with a radius of 100 mm and transmission of 2% at the laser wavelength was used as an output coupler (OC). The laser pulse trains were recorded by a 1 GHz digital oscilloscope (model MDO4104 C made by Tektronix in the USA) and a fast photodiode detector (model ET-5000 made by Electro-Optics Technology in the USA) with a rising time of 250 ps. A laser power meter (model 30 A-SH-V1 made by OPHIR in Israel) was used to measure the output power.

The diode-pumped Tm:YLF continuous-wave (CW) laser operation without GO was realized first. As shown in Fig. 3, the measured CW average output power increased linearly with the absorbed pump power. In order to protect the crystal, the maximum absorbed pump power was below 5.44 W in this experiment. The laser threshold (corresponding to the absorbed pump power)

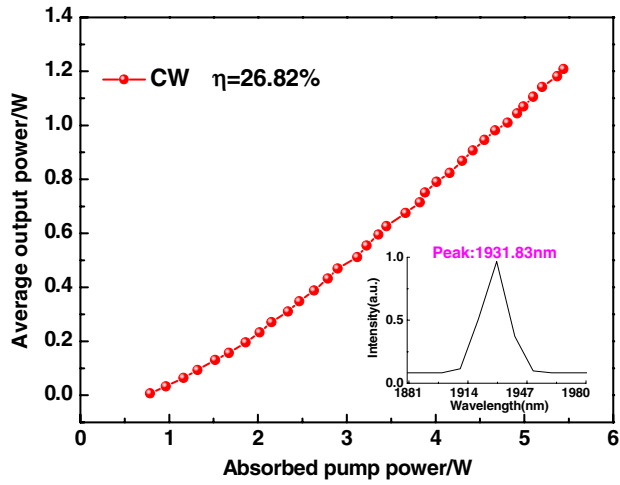


Fig. 3. Average output power as a function of absorbed pump power for CW and the inset shows the output spectrum of CW.

was 0.786 W. The maximum average output power of the CW laser was 1.209 W at an absorbed pumped power of 5.44 W, corresponding to the slope efficiency of 26.8%. The CW laser spectrum is shown in the inset of Fig. 3, with peak wavelength at about 1931.83 nm.

On inserting the GOSA close to the IM, the diode-pumped Tm:YLF laser ran into passively  $Q$ -switched operations. When the absorbed pump power reached 1.415 W, the  $Q$ -switched operation was stably observed by adjusting the angle and position of the absorber. As can be seen from this, the threshold value of the laser became slightly higher when compared with that of the cavity without GO. The measured average output power for the diode-pumped passively  $Q$ -switched Tm:YLF laser is shown in Fig. 4. When the absorbed pump power increased to 4.44 W, the maximum average output power of 379 mW was obtained, corresponding to the slope

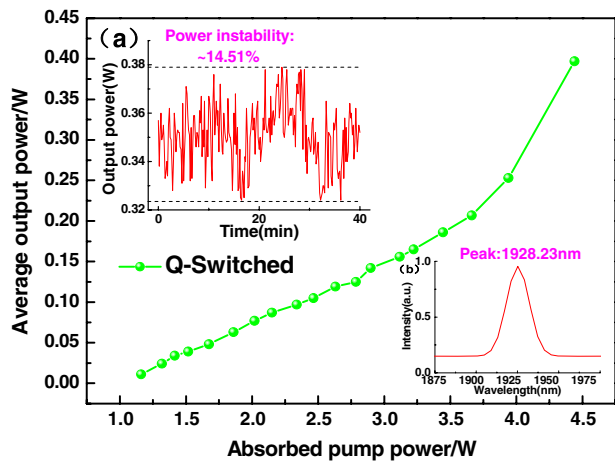
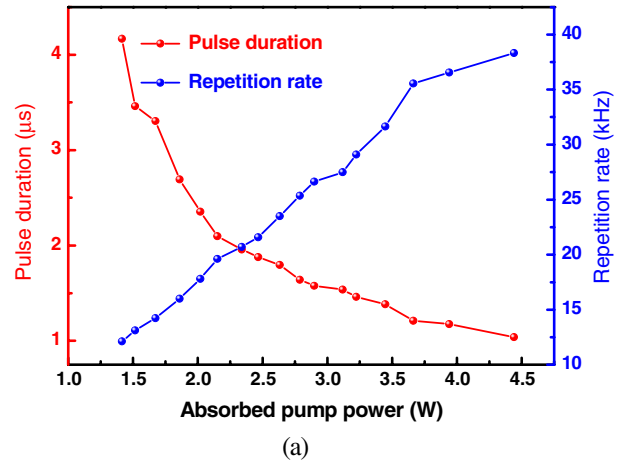


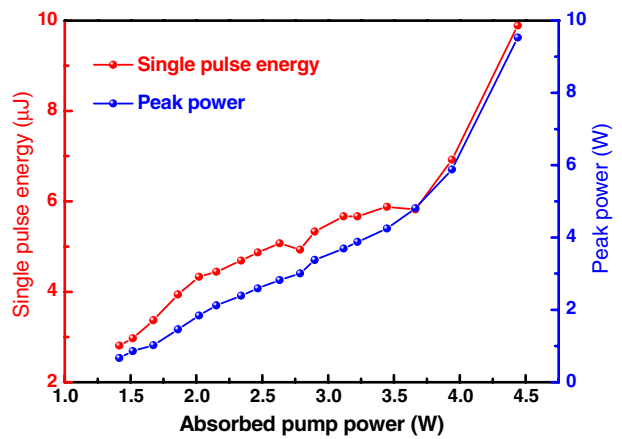
Fig. 4. Average output power of the GO  $Q$ -switched Tm:YLF laser. Inset (a) describes the output fluctuation versus time, and inset (b) displays the laser emission spectrum.

efficiency of 9.6%. As we continued to increase the pump power, the passively  $Q$ -switched operation started to become unstable. Then we decreased the pump power and the pulse train became stable again. That indicated the GO was not damaged. At the maximum output power, the output power fluctuation of the  $Q$ -switched laser was recorded for 40 min, as shown in inset (a) of Fig. 4. The power instability was  $\sim 14.5\%$ . The measured laser emission spectrum is shown in inset (b) of Fig. 4. The peak wavelength was located at 1928.23 nm.

The dependence of the pulse width and the pulse repetition rate of the  $Q$ -switched operation on the absorbed pump power is shown in Fig. 5(a). The single pulse energy and the peak power as functions of the absorbed pump power are shown in Fig. 5(b). It can be seen that the repetition rate, the single pulse energy, and the peak power increased, and the pulse width became narrower with the augments of absorbed pump power. This trend exhibited the typical feature of passively  $Q$ -switched pulses. When the absorbed pump power reached 4.44 W, the minimum pulse width was 1.038  $\mu\text{s}$  while the maximum repetition rate was 38.33 kHz, corresponding to the single pulse



(a)



(b)

Fig. 5. (a) Pulse duration and repetition rate versus absorbed pump power; (b) single pulse energy and peak power versus absorbed pump power.

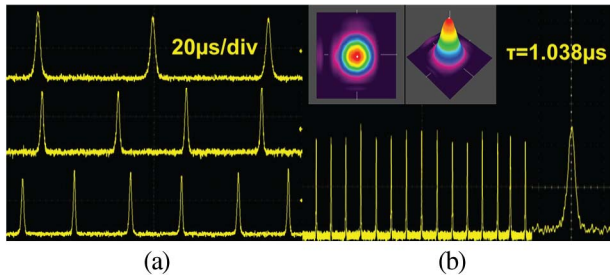


Fig. 6. (a)  $Q$ -switched pulse trains under absorbed pump powers of 2.957, 4.815, and 7.830 W; (b) a typical pulse profile of the  $Q$ -switched laser in different time scales and the inset displays the 2D and 3D images of the far-field intensity distribution for the  $Q$ -switched laser.

energy and peak power of 9.89  $\mu\text{J}$  and 9.53 W, respectively.

As shown in Fig. 6(a), typical passively  $Q$ -switched pulse trains were measured under different absorbed pump power. It can also be seen that the pulse width decreased with the increase of absorbed pump power at the same time scale. As shown in Fig. 6(b), a typical stable pulse profile (with the narrowest pulse width) of the passively  $Q$ -switched laser was displayed. The inset of Fig. 6(b) showed the 2D and 3D images of far-field intensity distribution for the  $Q$ -switched laser. These results indicate that the generated beam had an excellent TEM<sub>00</sub> transverse profile.

To express the condition for  $Q$ -switching, we quoted the formula<sup>[4]</sup>

$$-\frac{1}{T_R} I \frac{dq}{dI} > \frac{r}{\tau}, \quad (2)$$

where  $q$  is the saturable loss of the absorber,  $I$  is the laser intensity incident on the absorber,  $T_R$  is the cavity roundtrip time,  $r$  is the pump parameter that determines how many times the laser is pumped above the threshold, and  $\tau$  is the upper state lifetime of the gain medium. The long upper state lifetime for the Tm:YLF laser is 14 ms and the cavity length is 38 mm. Both are suitable for realizing the  $Q$ -switched operation in our experiment.

By using the GO as an SA, a compact stable passively  $Q$ -switched diode-pumped solid-state Tm:YLF laser at 2  $\mu\text{m}$  was experimentally demonstrated for the first time. The narrowest pulse width of 1.038  $\mu\text{s}$  and the maximum repetition rate of 38.33 kHz were obtained in our experiment. When the absorbed pump power increased to 4.44 W, the maximum average output power and the single pulse energy were 379 mW and 9.89  $\mu\text{J}$ , respectively. Our results reveal GO is suitable in 2  $\mu\text{m}$  diode-pumped lasers. In the future, we hope that the laser performance will be further improved by optimizing the design of the resonator, the pump source and the coupling system, and the parameters of SAs, and the continuous mode-locked pulse laser by GO would be expected.

This work was supported by the National Natural Science Foundation of China (No. 61475089); Development Projects of Shandong Province Science and Technology (No. 2017GGX30102).

## References

1. J. M. Serres, P. Loiko, X. Mateos, K. Yumashev, U. Griebner, V. Petrov, M. Aguiló, and F. Díaz, *Opt. Express* **23**, 14108 (2015).
2. C. Feng, D. H. Liu, and J. Liu, *J. Mod. Opt.* **59**, 1825 (2012).
3. Z. S. Qu, Y. G. Wang, J. Liu, L. H. Zheng, L. B. Su, and J. Xu, *Appl. Phys. B* **109**, 143 (2012).
4. Z. S. Qu, Y. G. Wang, J. Liu, L. H. Zheng, L. B. Su, and J. Xu, *Chin. Phys. B* **21**, 064211 (2012).
5. J. Liu, Y. G. Wang, Z. S. Qu, L. H. Zheng, L. B. Su, and J. Xu, *Laser Phys. Lett.* **9**, 15 (2012).
6. M. Segura, M. Kadankov, X. Mateos, A. Tyazhev, M. C. Pujol, J. J. Carvajal, M. Aguiló, F. Díaz, U. Griebner, and V. Petrov, *Opt. Express* **20**, 3394 (2012).
7. B. Oreshkov, S. Veronesi, M. Tonelli, A. D. Lieto, V. Petrov, U. Griebner, X. Mateos, and I. Buchvarov, *IEEE Photon. J.* **7**, 1 (2015).
8. J. L. Lan, Z. Y. Zhou, X. F. Guan, B. Xu, H. Y. Xu, Z. P. Cai, X. D. Xu, D. Z. Li, and J. Xu, *Opt. Mater. Express* **7**, 1725 (2017).
9. P. G. Ge, J. Liu, S. Z. Jiang, Y. Y. Xu, and B. Y. Man, *Photon. Res.* **3**, 256 (2015).
10. H. L. Wan, W. Cai, F. Wang, S. Z. Jiang, S. C. Xu, and J. Liu, *Opt. Quantum Electron.* **48**, 11 (2016).
11. Y. Q. Li, J. Liu, H. T. Zhu, L. H. Zheng, L. B. Su, J. Xu, and Y. G. Wang, *Opt. Commun.* **330**, 151 (2014).
12. A. Schmidt, D. Parisi, S. Veronesi, M. Tonelli, W. B. Cho, S. Y. Choi, J. H. Yim, S. Lee, F. Rotermund, U. Griebner, and V. Petrov, *CLEO: 2011 - Laser Science to Photonic Applications* (2011).
13. R. Frost, G. E. Jönsson, D. Chakarov, S. Svedhem, and B. Kasemo, *Nano Lett.* **12**, 3356 (2012).
14. J. Boguslawski, J. Sotor, G. Sobon, R. Kozinski, K. Librant, M. Aksienionek, L. Lipinska, and K. M. Abramski, *Photon. Res.* **3**, 119 (2015).
15. D. R. Cooper, B. D'Anjou, N. Ghattamaneni, B. Harack, M. Hilke, A. Horth, N. Majlis, M. Massicotte, L. Vandsburger, E. Whiteway, and V. Yu, *ISRN Condens. Matter Phys.* **2012**, 56 (2012).
16. W. Cai, S. Z. Jiang, S. C. Xu, Y. Q. Li, J. Liu, C. Li, L. H. Zheng, L. B. Su, and J. Xu, *Opt. Laser Technol.* **65**, 1 (2015).
17. H. T. Zhu, L. N. Zhao, J. Liu, S. C. Xu, W. Cai, S. Z. Jiang, L. H. Zheng, L. B. Su, and J. Xu, *Opt. Eng.* **55**, 081304 (2016).
18. W. Cai, Y. Q. Li, H. T. Zhu, S. Z. Jiang, S. C. Xu, J. Liu, L. H. Zheng, L. B. Su, and J. Xu, *Opt. Eng.* **53**, 126103 (2014).
19. Q. Song, G. J. Wang, B. Y. Zhang, W. J. Wang, M. H. Wang, Q. L. Zhang, G. H. Sun, Y. Bo, and Q. J. Peng, *Appl. Opt.* **54**, 2688 (2015).
20. Y. G. Wang, H. R. Chen, X. M. Wen, W. F. Hsieh, and J. Tang, *Nanotechnology* **22**, 455203 (2011).
21. F. Y. Zhao, Y. S. Wang, Y. G. Wang, H. S. Wang, and Y. J. Cai, *Chin. Opt. Lett.* **15**, 101402 (2017).
22. H. T. Zhu, W. Cai, J. F. Wei, J. Liu, L. H. Zheng, L. B. Su, J. Xu, and Y. G. Wang, *Opt. Laser Technol.* **68**, 120 (2015).
23. G. Eda and M. Chhowalla, *Adv. Mater.* **22**, 2392 (2010).
24. M. Jung, J. Koo, J. Park, Y. W. Song, Y. M. Jhon, K. Lee, S. Lee, and J. H. Lee, *Opt. Express* **21**, 20062 (2013).
25. G. Sobon, J. Sotor, I. Pasternak, A. Krajewska, W. Strupinski, and K. M. Abramski, *Opt. Mater. Express* **5**, 2884 (2015).
26. Y. G. Wang, Z. S. Qu, J. Liu, and Y. H. Tsang, *J. Lightwave Technol.* **30**, 3259 (2012).
27. X. M. Duan, B. Q. Yao, Y. J. Zhang, C. W. Song, Y. L. Ju, and Y. Z. Wang, *Chin. Opt. Lett.* **6**, 591 (2008).

28. Y. F. Dai, Y. Y. Li, X. Zou, B. X. Jiang, Y. Hang, and Y. X. Leng, *Opt. Laser Technol.* **57**, 202 (2014).
29. R. Faoro, M. Kadankov, D. Parisi, S. Veronesi, M. Tonelli, V. Petrov, U. Griebner, M. Segura, and X. Mateos, *Opt. Lett.* **37**, 1517 (2012).
30. H. Hecht, Z. Burshtein, A. Katzir, S. Noach, M. Sokol, E. Frumker, E. Galun, and A. A. Ishaaya, *Opt. Mater.* **64**, 64 (2017).
31. F. Canbaz, I. Yorulmaz, and A. Sennaroglu, *Opt. Lett.* **42**, 1656 (2017).
32. J. K. Jabczynski, L. Gorajek, W. Zendzian, J. Kwiatkowski, H. Jelinkova, J. Sulc, and M. Nemeč, *Adv. Solid-State Photon. WE44* (2008).
33. J. K. Jabczynski, J. Kwiatkowski, L. Gorajek, and W. Zendzian, in *Quantum Electronics and Laser Science Conference* (2008), paper JTua6.
34. J. K. Jabczynski, W. Zendzian, J. Kwiatkowski, H. Jelinkova, J. Sulc, and M. Nemeč, *Laser Phys. Lett.* **4**, 863 (2007).
35. Q. L. Bao, H. Zhang, Z. H. Ni, Y. Wang, L. Polavarapu, Z. X. Shen, Q. H. Xu, D. Y. Tang, and K. P. Loh, *Nano Res.* **4**, 297 (2011).
36. Y. J. Wu, C. Zhang, J. J. Liu, H. N. Zhang, J. M. Yang, and J. Liu, *Opt. Laser Technol.* **97**, 268 (2017).